J. Appl. Comput. Mech., 5(2) (2019) 367-380
DOI: 10.22055/JACM.2018.26739.1353

ISSN: 2383-4536
jacm.scu.ac.ir

M&MoCS
Shahid Chamran University of Ahvaz

Journal of Applied and Computational Mechanics

Research Paper

A New Quasi-3D Model for Functionally Graded Plates

Shantaram M. Ghumare[1], Atteshamuddin S. Sayyad[2]

[1] Department of Civil Engineering, SRES's Sanjivani College of Engineering, Savitribai Phule Pune University Kopargaon-423601, Maharashtra, India, smghumare@rediffmail.com

[2] Department of Civil Engineering, SRES's Sanjivani College of Engineering, Savitribai Phule Pune University Kopargaon-423601, Maharashtra, India, attu_sayyad@yahoo.co.in

Received August 08 2018; Revised September 29 2018; Accepted for publication October 01 2018.
Corresponding author: Atteshamuddin S. Sayyad, attu_sayyad@yahoo.co.in

Abstract. This article investigates the static behavior of functionally graded plate under mechanical loads by using a new quasi 3D model. The theory is designated as fifth-order shear and normal deformation theory (FOSNDT). Properties of functionally graded material are graded across the transverse direction by using the rule of mixture i.e. power-law. The effect of thickness stretching is considered to develop the present theory. In this theory, axial and transverse displacement components respectively involve fifth-order and fourth-order shape functions to evaluate shear and normal strains. The theory involves nine unknowns. Zero transverse shear stress conditions are satisfied by employing constitutive relations. Analytical solutions are obtained by implementing the double Fourier series technique. The results predicted by the FOSNDT are compared with existing results. It is pointed out that the present theory is helpful for accurate structural analysis of isotropic and functionally graded plates compared to other plate models.

Keywords: FOSNDT, FG plate, Static behavior, Shear deformation, Thickness stretching.

1. Introduction

Nowadays, functionally graded (FG) materials are being used in many advanced and important engineering structures. The material composition and volume fraction vary according to the simple rule of mixture i.e. power-law through the thickness. Wide applications of FGM in various industries forced researchers to develop accurate analytical and numerical techniques. This can be achieved by selecting a proper structural theory. Modeling of plate structures is based on either classical and refined computational models or three-dimensional elasticity theories. However, exact 3D elasticity theories for the FG plates are not found in the whole variety of literature. Therefore, researchers have hired various approximate plate theories for predicting the structural behavior of FG plates. Approximate theories reduce the 3D problem to a 2D problem. Various investigations on FG plate which are based on approximate theories are well documented in Jha et al. [1], Swaminathan et al. [2], Swaminathan and Sangeeta [3], etc.

Classical plate theory (CPT) predicts zero values for strains in the transverse direction (*z*-direction). Therefore, it is not suitable for thick FG plates wherein these strains are more pronounced. The first-order shear deformation theory (FSDT) considered these strain components, but shows constant variation of transverse strains in the transverse direction. These drawbacks of CPT and FSDT forced the researchers to develop refined plate theories. Several higher-order shear deformation theories (HSDTs) are developed by different scientists for predicting the structural behavior of FG plates. These theories are systematically documented by Sayyad and Ghugal [4, 5]. Reddy [6] analyzed the FG plates by his well-known polynomial type model. Reddy and Cheng [7] presented 3D asymptotic theory for FG plates. Zenkour [8] studied the behavior of FG plates under uniform load. Zhong and Shang [9] presented 3D analysis of FG plates using Plevako's solution. Lu et al. [10] obtained natural frequencies of FG thick plates using 3D elasticity theory. Ameur et al. [11] developed a trigonometric theory containing

Published online: March 21 2019

four unknowns for the bending of FG plates. Jha et al. [12] and Neves et al. [13] presented stress solutions for FG plates based on HSDT with including normal deformation.

Thai and Choi [14] attempted buckling analysis of FG plates by utilizing a refined model. Second-degree variation of the shear strains in the transverse direction is accounted. Najafizadeh et al. [15] investigated frequencies of FG plates with non-ideal end conditions. Neves et al. [16] addressed flexure and vibration problems of FG plates by deploying hyperbolic theory. Thai and Thuc [17] and Thai and Kim [18] tried new theories for flexure, buckling, and vibration of FG plates. Mechab et al. [19] obtained solutions for flexure conditions of functionally graded plates by employing the refined theory. Thai and Choi [20] developed a FEM solution for FG plates. Reddy and Kant [21] determined frequencies for FG plates made of exponentially graded materials using 3D exact solution. Thai and Choi [22] obtained an analytical solution hiring Levy's solution technique to determine frequencies for FG plates with different end conditions based on a refined theory. H adji et al. [23] developed a HSDT model for static and vibration problems of FG beams. Mantari et al. [24] have used five non-polynomial displacement based theories for FG plates. Amirpour et al. [25] have utilized HSDT for thick FG plates with varying stiffness. Thai et al. [26] presented a theory for FG plates containing four unknowns. Li and Zhang [27] reported the vibration study on FG plate with rotation. Park and Choi [28] developed a simple FSDT for predicting the global respo nse of isotropic plates. Sayyad and Ghugal [29] presented a unified shear deformation theory for FG beams and plates. Naik and Sayyad [30] developed higher-order plate theory for the cylindrical bending problem of plates. Sayyad and Ghugal [31] have reviewed the literature on the analysis of FG sandwich beams by means of refined beam theories based on the analytical and numerical techniques.

Recently, few research papers have been published on the applications of analytical [32-38] and numerical methods [39-50] for the analysis of functionally graded beams, plates, and shells. However, in most of the literature, the effect of transverse normal deformation is neglected to minimize unknown variables in the displacement field.

1.1 Present Contribution

In the current contribution, FOSNDT investigated by Ghumare and Sayyad [51] is extended to examine structural behavior of the FG plates under transverse loadings. The novelty and contribution of the present theory are summarized as follows:

1) For the accurate description of the bending behavior of the thick FGM plates, shear and normal deformations play important roles. Thus, their effects are considered. Many published theories neglect the effect of transverse normal deformations. Hence, in this work, a new quasi-3D model is presented for FG plate including normal deformation along with shear deformation.
2) To account for the effects of cross-sectional warping and thickness stretching, a polynomial type shearing strain function expanded up to fifth-order is chosen. Zero transverse shear stress conditions are satisfied by using constitutive relations.
3) Since the current developed theory is a polynomial type, it is computationally simpler than non-polynomial plate theories which are mathematically more cumbersome.
4) Since 3D Hooke's law is used to obtained stresses associated with the present theory, it accurately describes the state of stress in 3D continuum.
5) The developed theory shows improvements in results when compared to the other HSDTs found in the literature [52-57].

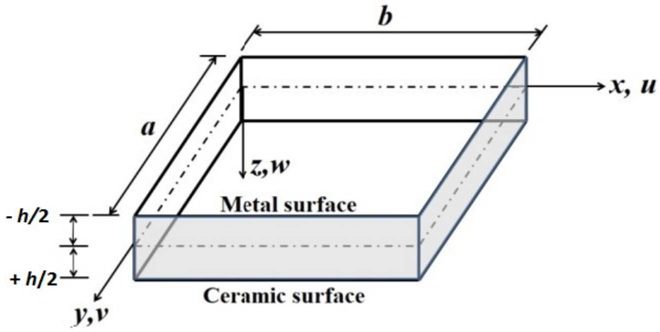

Fig. 1. FGM plate and its geometry with coordinates

2. Problem Formulation

The transversely loaded FG plate which is presented in Fig. 1 is considered for the mathematical formulation and numerical study. Properties of material graded in z-direction using the power-law relation stated in Eq. (1), wherein top face is made of metal and bottom face is of purely ceramic.

$$E(z) = E_m V_m + E_c V_c, \quad V_m = 1 - V_c \quad V_c = (0.5 + z/h)^P \tag{1}$$

where subscript ***m*** stands for metal and subscript ***c*** refers to ceramic. ***E*** is the elastic modulus, ***V*** is the volume fraction, and ***P*** is the power-law coefficient/index. Fig. 2 plots the elastic modulus in z-direction.

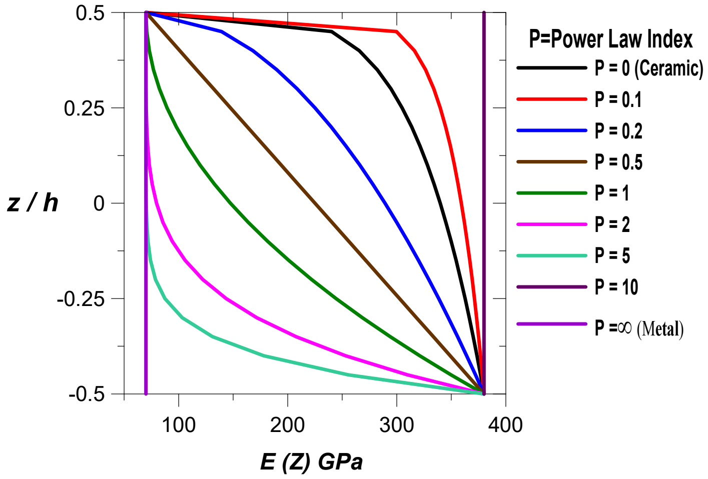

Fig. 2. Variation of elastic modulus in z-direction

2.1 Kinematics of the present model

The displacement field of the present theory is defined as,

$$\begin{aligned} u &= u_0 - z\frac{\partial w_0}{\partial x} + z\left[1-\frac{4}{3}\frac{z^2}{h^2}\right]\phi_x + z\left[1-\frac{16}{5}\frac{z^4}{h^4}\right]\psi_x \\ v &= v_0 - z\frac{\partial w_0}{\partial y} + z\left[1-\frac{4}{3}\frac{z^2}{h^2}\right]\phi_y + z\left[1-\frac{16}{5}\frac{z^4}{h^4}\right]\psi_y \\ w &= w_0 + \left[1-4\frac{z^2}{h^2}\right]\phi_z + \left[1-16\frac{z^4}{h^4}\right]\psi_z \end{aligned} \tag{2}$$

where u_0, v_0, w_0 are the displacements of a mid-plane. $\phi_x, \psi_x, \phi_y, \psi_y, \phi_z, \psi_z$ are the unknown rotations. $f_1(z)$ and $f_2(z)$ are assumed to get the parabolic variation of shear strains. The non-zero normal and shear strain ($\varepsilon_x, \varepsilon_y, \varepsilon_z, \gamma_{xz}, \gamma_{yz}, \gamma_{xy}$) components are as follows:

$$\begin{aligned} \varepsilon_x &= \varepsilon_x^0 + z\,k_x^b + \left[z-(4/3)(z^3/h^2)\right]\varepsilon_x^1 + \left[z-(16/5)(z^5/h^4)\right]\varepsilon_x^2 \\ \varepsilon_y &= \varepsilon_y^0 + z\,k_y^b + \left[z-(4/3)(z^3/h^2)\right]\varepsilon_y^1 + \left[z-(16/5)(z^5/h^4)\right]\varepsilon_y^2 \\ \varepsilon_z &= \left(-8z/h^2\right)\phi_z + \left[z\left(-64z^3/h^4\right)\right]\psi_z \\ \gamma_{xy} &= \gamma_{xy}^0 + z\,k_{xy}^b + \left[z-(4/3)(z^3/h^2)\right]\gamma_{xy}^1 + \left[z-(16/5)(z^5/h^4)\right]\gamma_{xy}^2 \\ \gamma_{xz} &= \left[1-4\left(z^2/h^2\right)\right]\gamma_{xz}^{s_1} + \left[z\left(1-16(z^3/h^4)\right)\right]\gamma_{xz}^{s_2} \\ \gamma_{yz} &= \left[1-4\left(z^2/h^2\right)\right]\gamma_{yz}^{s_1} + \left[z\left(1-16(z^3/h^4)\right)\right]\gamma_{yz}^{s_2} \end{aligned} \tag{3}$$

where

$$\begin{aligned} &\varepsilon_x^0 = \frac{\partial u_0}{\partial x},\ k_x^b = -\frac{\partial^2 w_0}{\partial x^2},\ \varepsilon_x^1 = \frac{\partial \phi_x}{\partial x},\ \varepsilon_x^2 = \frac{\partial \psi_x}{\partial x},\ \varepsilon_y^0 = \frac{\partial v_0}{\partial y},\ k_y^b = -\frac{\partial^2 w_0}{\partial y^2},\ \varepsilon_y^1 = \frac{\partial \phi_y}{\partial y}, \\ &\varepsilon_y^2 = \frac{\partial \psi_y}{\partial y},\ \gamma_{xy}^{s_1} = \left(\phi_x + \frac{\partial \phi_y}{\partial y}\right),\ \gamma_{xy}^{s_2} = \left(\psi_x + \frac{\partial \psi_y}{\partial y}\right), \gamma_{yz}^{s_1} = \left(\phi_y + \frac{\partial \phi_z}{\partial z}\right),\ \gamma_{yz}^{s_2} = \left(\psi_y + \frac{\partial \psi_z}{\partial z}\right), \\ &\gamma_{xz}^{s_1} = \left(\phi_x + \frac{\partial \phi_z}{\partial x}\right),\ \gamma_{xz}^{s_2} = \left(\psi_x + \frac{\partial \psi_z}{\partial x}\right) \end{aligned} \tag{4}$$

2.2 Constitutive relation

The stresses are obtained using the 3D constitutive relations stated in Eq. (5)

$$\begin{Bmatrix} \sigma_x \\ \sigma_y \\ \sigma_z \\ \tau_{xy} \\ \tau_{xz} \\ \tau_{yz} \end{Bmatrix} = \begin{bmatrix} Q_{11} & Q_{12} & Q_{13} & 0 & 0 & 0 \\ Q_{12} & Q_{22} & Q_{23} & 0 & 0 & 0 \\ Q_{13} & Q_{23} & Q_{33} & 0 & 0 & 0 \\ 0 & 0 & 0 & Q_{66} & 0 & 0 \\ 0 & 0 & 0 & 0 & Q_{44} & 0 \\ 0 & 0 & 0 & 0 & 0 & Q_{55} \end{bmatrix} \begin{Bmatrix} \varepsilon_x \\ \varepsilon_y \\ \varepsilon_z \\ \gamma_{xy} \\ \gamma_{xz} \\ \gamma_{yz} \end{Bmatrix} \tag{5}$$

where

$$\begin{gathered} Q_{11} = Q_{22} = Q_{33} = \frac{E(z)\,(1-\mu)}{(1+\mu)\,(1-2\mu)} \\ Q_{12} = Q_{13} = Q_{21} = Q_{23} = Q_{31} = Q_{32} = \frac{E(z)\,\mu}{(1+\mu)(1-2\mu)} \\ Q_{44} = Q_{55} = Q_{66} = \frac{E(z)}{2(1+\mu)} \end{gathered} \tag{6}$$

2.3 Governing differential equations

The principle of virtual work stated in Eq. (7) is applied to derive the variationally consistent governing differential equations.

$$\int_0^a \int_0^b \int_{-h/2}^{h/2} \begin{pmatrix} \sigma_x \delta\varepsilon_x + \sigma_y \delta\varepsilon_y + \sigma_z \delta\varepsilon_z \\ + \tau_{xy}\delta\,\gamma_{xy} + \tau_{xz}\delta\,\gamma_{xz} + \tau_{yz}\delta\,\gamma_{yz} \end{pmatrix} dz\,dy\,dx = \int_0^a \int_0^b q(x,y)\,\delta w\,dy\,dx \tag{7}$$

where δ represents the variational operator. Substituting non-zero strains from Eqs. (3) and (4) into Eq. (7) one can write:

$$\begin{aligned} &\int_0^a \int_0^b \Bigg(N_x \frac{\partial \delta u_0}{\partial x} - M_x^b \frac{\partial^2 \delta w_0}{\partial x^2} + M_x^{S_1} \frac{\partial \delta \phi_x}{\partial x} + M_x^{S_2} \frac{\partial \delta \psi_x}{\partial x} + N_y \frac{\partial \delta v_0}{\partial y} - M_y^b \frac{\partial^2 w_0}{\partial y^2} + M_y^{S_1} \frac{\partial \delta \phi_y}{\partial y} \\ &+ M_y^{S_2} \frac{\partial \delta \psi_y}{\partial x} + Q_z^1 \delta\phi_z + Q_z^2 \delta\psi_z + N_{xy} \frac{\partial \delta u_0}{\partial y} + N_{xy} \frac{\partial \delta v_0}{\partial x} - 2M_{xy}^b \frac{\partial^2 \delta w_0}{\partial x \partial y} + M_{xy}^{S_1} \frac{\partial \delta \phi_x}{\partial y} + M_{xy}^{S_1} \frac{\partial \delta \phi_y}{\partial x} \\ &+ M_{xy}^{S_2} \frac{\partial \delta \psi_x}{\partial y} + M_{xy}^{S_2} \frac{\partial \delta \psi_y}{\partial x} + Q_{xz}^1 \left[\delta\phi_x + \frac{\partial \delta \phi_z}{\partial x} \right] + Q_{xz}^2 \left[\delta\psi_x + \frac{\partial \delta \psi_z}{\partial x} \right] + Q_{yz}^1 \left[\delta\phi_y + \frac{\partial \delta \phi_z}{\partial y} \right] + \\ &Q_{yz}^2 \left[\delta\psi_y + \frac{\partial \delta \psi_z}{\partial y} \right] dy\,dx = \int_0^a \int_0^b q(x,y)\,\delta w\,dy\,dx \end{aligned} \tag{8}$$

here

$$\begin{gathered} N_x = \int_{-h/2}^{+h/2} \sigma_x\,dz, \quad M_x^b = \int_{-h/2}^{+h/2} \sigma_x\,z\,dz, \quad M_x^{S_1} = \int_{-h/2}^{+h/2} \sigma_x \left[z - (4/3)(z^3/h^2) \right] dz, \\ M_x^{S_2} = \int_{-h/2}^{+h/2} \sigma_x \left[z - (16/5)(z^5/h^4) \right] dz, \quad N_y = \int_{-h/2}^{+h/2} \sigma_y\,dz, \quad M_y^b = \int_{-h/2}^{+h/2} \sigma_y\,z\,dz, \\ M_y^{S_1} = \int_{-h/2}^{+h/2} \sigma_y \left[z - (4/3)(z^3/h^2) \right] dz, \quad M_y^{S_2} = \int_{-h/2}^{+h/2} \sigma_y \left[z - (16/5)(z^5/h^4) \right] dz, \\ N_{xy} = \int_{-h/2}^{+h/2} \tau_{xy}\,dz, \quad M_{xy}^b = \int_{-h/2}^{+h/2} \tau_{xy}\,z\,dz, \quad M_{xy}^{S_1} = \int_{-h/2}^{+h/2} \tau_{xy} \left[z - (4/3)(z^3/h^2) \right] dz, \\ M_{xy}^{S_2} = \int_{-h/2}^{+h/2} \tau_{xy} \left[z - (16/5)(z^5/h^4) \right] dz, \quad Q_{xz}^1 = \int_{-h/2}^{+h/2} \tau_{xz} \left[1 - 4(z^2/h^2) \right] dz, \\ Q_{xz}^2 = \int_{-h/2}^{+h/2} \tau_{xz} \left[z\left(1 - 16(z^3/h^4)\right) \right] dz, \quad Q_{yz}^1 = \int_{-h/2}^{+h/2} \tau_{yz} \left[1 - 4(z^2/h^2) \right] dz, \\ Q_{yz}^2 = \int_{-h/2}^{+h/2} \tau_{yz} \left[z\left(1 - 16(z^3/h^4)\right) \right] dz, \quad Q_z^1 = \int_{-h/2}^{+h/2} \sigma_Z \left(-8z/h^2\right) dz, \quad Q_z^2 = \int_{-h/2}^{+h/2} \sigma_y \left[z\left(-64z^3/h^4\right) \right] dz \end{gathered} \tag{9}$$

where, (N, M, Q) are the resultant in-plane forces, moments, and shear forces, respectively. The superscript ***b*** is associated with the terms analogous to classical theory, whereas S_1 and S_2 are the superscripts associated with the transverse shear deformation effect. Additionally, Superscripts 1 and 2 are associated with the shearing strain functions $f_1(z)$ and $f_2(z)$. The governing differential equations are obtained by integration of Eq. (8) and setting the coefficients of unknown equal to zero.

$$\delta u_0:\frac{\partial N_x}{\partial x}+\frac{\partial N_{xy}}{\partial y}=A_{11}\frac{\partial^2 u_0}{\partial x^2}-B_{11}\frac{\partial^3 w_0}{\partial x^3}+C_{11}\frac{\partial^2 \phi_x}{\partial x^2}+D_{11}\frac{\partial^2 \psi_x}{\partial x^2}+A_{12}\frac{\partial^2 v_0}{\partial x\partial y}-B_{12}\frac{\partial^3 w_0}{\partial x\partial y^2}+C_{12}\frac{\partial^2 \phi_y}{\partial x\partial y}+D_{12}\frac{\partial^2 \psi_y}{\partial x\partial y}$$
$$+I_{13}\frac{\partial \phi_Z}{\partial x}+J_{13}\frac{\partial \psi_Z}{\partial x}+A_{66}\frac{\partial^2 u_0}{\partial y^2}+A_{66}\frac{\partial^2 v_0}{\partial x\partial y}-2B_{66}\frac{\partial^3 w_0}{\partial x\partial y^2}+C_{66}\frac{\partial^2 \phi_x}{\partial y^2}+C_{66}\frac{\partial^2 \phi_y}{\partial x\partial y}+D_{66}\frac{\partial^2 \psi_x}{\partial y^2}+C_{66}\frac{\partial^2 \psi_y}{\partial x\partial y}=0 \tag{10}$$

$$\delta v_0:\frac{\partial N_y}{\partial y}+\frac{\partial N_{xy}}{\partial x}=A_{12}\frac{\partial^2 u_0}{\partial x\partial y}-B_{12}\frac{\partial^3 w_0}{\partial x^2\partial y}+C_{12}\frac{\partial^2 \phi_x}{\partial x\partial y}+D_{12}\frac{\partial^2 \psi_x}{\partial x\partial y}+A_{22}\frac{\partial^2 v_0}{\partial y^2}-B_{22}\frac{\partial^3 w_0}{\partial y^3}+C_{22}\frac{\partial^2 \phi_y}{\partial y^2}+D_{22}\frac{\partial^2 \psi_y}{\partial y^2}$$
$$+I_{23}\frac{\partial \phi_Z}{\partial y}+J_{23}\frac{\partial \psi_Z}{\partial y}+A_{66}\frac{\partial^2 u_0}{\partial x\partial y}+A_{66}\frac{\partial^2 v_0}{\partial x^2}-2B_{66}\frac{\partial^3 w_0}{\partial x^2\partial y}+C_{66}\frac{\partial^2 \phi_x}{\partial x\partial y}+C_{66}\frac{\partial^2 \phi_y}{\partial x^2}+D_{66}\frac{\partial^2 \psi_x}{\partial x\partial y}+C_{66}\frac{\partial^2 \psi_y}{\partial x^2}=0 \tag{11}$$

$$\delta w_0:\frac{\partial^2 M_x^b}{\partial x^2}+\frac{\partial^2 M_y^b}{\partial y^2}+2\frac{\partial^2 M_{xy}^b}{\partial x\partial y}=B_{11}\frac{\partial^3 u_0}{\partial x^3}-A_{S11}\frac{\partial^4 w_0}{\partial x^4}+C_{S11}\frac{\partial^3 \phi_x}{\partial x^3}+D_{S11}\frac{\partial^3 \psi_x}{\partial x^3}+B_{12}\frac{\partial^3 v_0}{\partial x^2\partial y}-A_{S12}\frac{\partial^4 w_0}{\partial x^2\partial y^2}+C_{S12}\frac{\partial^3 \phi_y}{\partial x^2\partial y}$$
$$+D_{S12}\frac{\partial^3 \psi_y}{\partial x^2\partial y}+I_{S13}\frac{\partial^2 \phi_Z}{\partial x^2}+J_{S13}\frac{\partial^2 \psi_Z}{\partial x^2}+B_{12}\frac{\partial^3 u_0}{\partial x\partial y^2}-A_{S12}\frac{\partial^4 w_0}{\partial x^2\partial y^2}+C_{S12}\frac{\partial^3 \phi_x}{\partial x\partial y^2}+D_{S12}\frac{\partial^3 \psi_x}{\partial x\partial y^2}+B_{22}\frac{\partial^3 v_0}{\partial y^3}-A_{S22}\frac{\partial^4 w_0}{\partial y^4}$$
$$+C_{S22}\frac{\partial^3 \phi_y}{\partial y^3}+D_{S22}\frac{\partial^3 \psi_y}{\partial y^3}+I_{S23}\frac{\partial^2 \phi_Z}{\partial y^2}+J_{S23}\frac{\partial^2 \psi_Z}{\partial y^2}+2B_{66}\frac{\partial^3 u_0}{\partial x\partial y^2}+2B_{66}\frac{\partial^3 v_0}{\partial x^2\partial y}-4A_{S66}\frac{\partial^4 w_0}{\partial x^2\partial y^2}+2C_{S66}\frac{\partial^3 \phi_x}{\partial x\partial y^2}+2C_{S66}\frac{\partial^3 \phi_x}{\partial x\partial y^2}$$
$$+2D_{S66}\frac{\partial^3 \psi_x}{\partial x\partial y^2}+2D_{S66}\frac{\partial^3 \psi_y}{\partial x^2\partial y}=-q \tag{12}$$

$$\delta\phi_x:\frac{\partial M_x^{S_1}}{\partial x}+\frac{\partial M_{xy}^{S_1}}{\partial y}-Q_{xz}^1=C_{11}\frac{\partial^2 u_0}{\partial x^2}-C_{S11}\frac{\partial^3 w_0}{\partial x^3}+C_{SS111}\frac{\partial^2 \phi_x}{\partial x^2}+C_{SS211}\frac{\partial^2 \psi_x}{\partial x^2}+C_{12}\frac{\partial^2 v_0}{\partial x\partial y}-C_{S12}\frac{\partial^3 w_0}{\partial x\partial y^2}+C_{SS112}\frac{\partial^2 \phi_y}{\partial x\partial y}$$
$$+C_{SS212}\frac{\partial^2 \psi_y}{\partial x\partial y}+I_{SS113}\frac{\partial \phi_Z}{\partial x}+J_{SS113}\frac{\partial \psi_Z}{\partial x}+C_{66}\frac{\partial^2 u_0}{\partial y^2}-C_{66}\frac{\partial^2 v_0}{\partial x\partial y}-2C_{S66}\frac{\partial^3 w_0}{\partial x\partial y^2}+C_{SS166}\frac{\partial^2 \phi_x}{\partial y^2}+C_{SS166}\frac{\partial^2 \phi_y}{\partial x\partial y}+C_{SS266}\frac{\partial^2 \psi_x}{\partial y^2}$$
$$+C_{SS266}\frac{\partial^2 \psi_y}{\partial x\partial y}-C_{SSS144}\phi_x-C_{SSS144}\frac{\partial \phi_z}{\partial x}-C_{SSS244}\psi_x-C_{SSS244}\phi_x\frac{\partial \psi_z}{\partial x}=0 \tag{13}$$

$$\delta\psi_x:\frac{\partial M_x^{S_2}}{\partial x}+\frac{\partial M_{xy}^{S_2}}{\partial y}-Q_{xz}^2=D_{11}\frac{\partial^2 u_0}{\partial x^2}-D_{S11}\frac{\partial^3 w_0}{\partial x^3}+C_{SS211}\frac{\partial^2 \phi_x}{\partial x^2}+D_{SS211}\frac{\partial^2 \psi_x}{\partial x^2}+D_{12}\frac{\partial^2 v_0}{\partial x\partial y}-D_{S12}\frac{\partial^3 w_0}{\partial x\partial y^2}+C_{SS212}\frac{\partial^2 \phi_y}{\partial x\partial y}$$
$$+D_{SS212}\frac{\partial^2 \psi_y}{\partial x\partial y}+I_{SS213}\frac{\partial \phi_Z}{\partial x}+J_{SS213}\frac{\partial \psi_Z}{\partial x}+D_{66}\frac{\partial^2 u_0}{\partial y^2}+D_{66}\frac{\partial^2 v_0}{\partial x\partial y}-2D_{S66}\frac{\partial^3 w_0}{\partial x\partial y^2}+C_{SS266}\frac{\partial^2 \phi_z}{\partial y^2}+C_{SS266}\frac{\partial^2 \phi_y}{\partial x\partial y}+D_{SS266}\frac{\partial^2 \psi_x}{\partial y^2}$$
$$+C_{SS266}\frac{\partial^2 \psi_y}{\partial x\partial y}-C_{SSS244}\phi_x-C_{SSS244}\frac{\partial \phi_z}{\partial x}-D_{SSS244}\psi_x-D_{SSS244}\frac{\partial \psi_z}{\partial x}=0 \tag{14}$$

$$\delta\phi_y:\frac{\partial M_y^{S_1}}{\partial y}+\frac{\partial M_{xy}^{S_1}}{\partial x}-Q_{yz}^1=C_{12}\frac{\partial^2 u_0}{\partial x\partial y}-C_{S12}\frac{\partial^3 w_0}{\partial x^2\partial y}+C_{SS112}\frac{\partial^2 \phi_x}{\partial x\partial y}+C_{SS212}\frac{\partial^2 \psi_x}{\partial x\partial y}+C_{22}\frac{\partial^2 v_0}{\partial y^2}-C_{S22}\frac{\partial^3 w_0}{\partial y^3}$$
$$+C_{SS122}\frac{\partial^2 \phi_y}{\partial y^2}+C_{SS222}\frac{\partial^2 \psi_y}{\partial y^2}+I_{SS123}\phi_Z+J_{SS123}\psi_Z+C_{66}\frac{\partial^2 u_0}{\partial y^2}+C_{66}\frac{\partial^2 v_0}{\partial x\partial y}-2C_{S66}\frac{\partial^3 w_0}{\partial x^2\partial y}+C_{SS166}\frac{\partial^2 \phi_x}{\partial x\partial y}$$
$$+C_{SS166}\frac{\partial^2 \phi_y}{\partial x^2}+C_{SS266}\frac{\partial^2 \psi_x}{\partial x\partial y}+C_{SS266}\frac{\partial^2 \psi_y}{\partial x^2}-C_{SSS155}\phi_y-C_{SSS155}\frac{\partial \phi_z}{\partial y}-C_{SSS255}\psi_y-C_{SSS255}\frac{\partial \psi_z}{\partial y}=0 \tag{15}$$

$$\delta\psi_y:\frac{\partial M_y^{S_2}}{\partial y}+\frac{\partial M_{xy}^{S_2}}{\partial x}-Q_{yz}^2=D_{12}\frac{\partial^2 u_0}{\partial x\partial y}-D_{S12}\frac{\partial^3 w_0}{\partial x^2\partial y}+C_{SS212}\frac{\partial^2 \phi_x}{\partial x\partial y}+D_{SS212}\frac{\partial^2 \psi_x}{\partial x\partial y}+D_{22}\frac{\partial^2 v_0}{\partial y^2}-D_{S22}\frac{\partial^3 w_0}{\partial y^3}$$
$$+C_{SS222}\frac{\partial^2 \phi_y}{\partial y^2}+D_{SS222}\frac{\partial^2 \psi_y}{\partial y^2}+I_{SS223}\frac{\partial \phi_Z}{\partial y}+J_{SS223}\frac{\partial \psi_Z}{\partial y}+D_{66}\frac{\partial^2 u_0}{\partial x\partial y}+D_{66}\frac{\partial^2 v_0}{\partial x^2}-2D_{S66}\frac{\partial^3 w_0}{\partial x^2\partial y}+C_{SS266}\frac{\partial^2 \phi_x}{\partial x\partial y}$$
$$+C_{SS266}\frac{\partial^2 \phi_y}{\partial y^2}+D_{SS266}\frac{\partial^2 \psi_x}{\partial x\partial y}+D_{SS266}\frac{\partial^2 \psi_y}{\partial x^2}-C_{SSS255}\phi_y-C_{SSS255}\frac{\partial \phi_z}{\partial y}-D_{SSS255}\psi_y-D_{SSS255}\frac{\partial \psi_z}{\partial y}=0 \tag{16}$$

$$\delta\phi_z:\ \frac{\partial Q_{xz}^1}{\partial x}+\frac{\partial Q_{yz}^1}{\partial y}-Q_z^1=C_{SSS144}\phi_x+C_{SSS144}\frac{\partial^2\phi_z}{\partial x^2}+C_{SSS244}\frac{\partial\psi_x}{\partial x}+C_{SSS244}\frac{\partial^2\psi_z}{\partial x^2}+C_{SSS155}\frac{\partial\phi_x}{\partial y}+C_{SSS155}\frac{\partial^2\phi_z}{\partial y^2}$$
$$+C_{SSS255}\frac{\partial\psi_y}{\partial y}+C_{SSS255}\frac{\partial^2\psi_z}{\partial y^2}-I_{13}\frac{\partial u_0}{\partial x}+I_{S13}\frac{\partial^2 w_0}{\partial x^2}-I_{SS113}\frac{\partial\phi_x}{\partial x}-I_{SS213}\frac{\partial\psi_x}{\partial x}-I_{23}\frac{\partial v_0}{\partial y}+I_{S23}\frac{\partial^2 w_0}{\partial y^2}-I_{SS123}\frac{\partial\phi_y}{\partial y} \tag{17}$$
$$-I_{SS223}\frac{\partial\psi_y}{\partial y}-I_{SSS133}\phi_z-I_{SSS233}\psi_z=0$$

$$\delta\psi_z:\ \frac{\partial Q_{xz}^2}{\partial x}+\frac{\partial Q_{yz}^2}{\partial y}-Q_z^2=C_{SSS244}\frac{\partial\phi_x}{\partial x}+C_{SSS244}\frac{\partial^2\phi_z}{\partial x^2}+D_{SSS244}\frac{\partial\psi_x}{\partial x}+D_{SSS244}\frac{\partial^2\psi_z}{\partial x^2}+C_{SSS255}\frac{\partial\phi_y}{\partial y}+C_{SSS255}\frac{\partial^2\phi_z}{\partial y^2}$$
$$+D_{SSS255}\frac{\partial\psi_y}{\partial y}+D_{SSS255}\frac{\partial^2\psi_z}{\partial y^2}-J_{13}\frac{\partial u_0}{\partial x}+J_{S13}\frac{\partial^2 w_0}{\partial x^2}-J_{SS113}\frac{\partial\phi_x}{\partial x}-J_{SS213}\frac{\partial\psi_x}{\partial x}-J_{23}\frac{\partial v_0}{\partial y}+J_{S23}\frac{\partial^2 w_0}{\partial y^2}-J_{SS123}\frac{\partial\phi_y}{\partial y} \tag{18}$$
$$-J_{SS223}\frac{\partial\psi_y}{\partial y}-I_{SSS233}\phi_z-J_{SSS233}\psi_z=0$$

where

$$A_{ij}=Q_{ij}\int_{+h/2}^{-h/2}dz,\quad B_{ij}=Q_{ij}\int_{+h/2}^{-h/2}z\,dz,\quad A_{Sij}=Q_{ij}\int_{+h/2}^{-h/2}z^2\,dz,$$
$$C_{ij}=Q_{ij}\int_{+h/2}^{-h/2}\left[z-(4/3)(z^3/h^2)\right]dz,\quad C_{Sij}=Q_{ij}\int_{+h/2}^{-h/2}z\left[z-(4/3)(z^3/h^2)\right]dz,$$
$$C_{SS1ij}=Q_{ij}\int_{+h/2}^{-h/2}\left[z-(4/3)(z^3/h^2)\right]\left[z-(16/5)(z^5/h^4)\right]dz,$$
$$C_{SS2ij}=Q_{ij}\int_{+h/2}^{-h/2}\left[z-(4/3)(z^3/h^2)\right]\left[z-(16/5)(z^5/h^4)\right]dz,$$
$$C_{SSS1ij}=Q_{ij}\int_{+h/2}^{-h/2}\left[1-4(z^2/h^2)\right]^2dz,\quad D_{ij}=Q_{ij}\int_{+h/2}^{-h/2}\left[z-(16/5)(z^5/h^4)\right]dz$$
$$C_{SSS2ij}=Q_{ij}\int_{+h/2}^{-h/2}\left[1-4(z^2/h^2)\right]\left[z(1-16(z^3/h^4))\right]dz,$$
$$D_{sij}=Q_{ij}\int_{+h/2}^{-h/2}z\left[z-(16/5)(z^5/h^4)\right]dz,\quad D_{ss2ij}=Q_{ij}\int_{+h/2}^{-h/2}\left[z-(16/5)(z^5/h^4)\right]^2dz,$$
$$D_{sss2ij}=Q_{ij}\int_{+h/2}^{-h/2}\left[z-(16/5)(z^5/h^4)\right]^2dz,\quad I_{ij}=Q_{ij}\int_{+h/2}^{-h/2}(-8z/h^2)dz,$$
$$I_{Sij}=Q_{ij}\int_{+h/2}^{-h/2}z(-8z/h^2)dz,\quad I_{SS1ij}=Q_{ij}\int_{+h/2}^{-h/2}\left[z-(4/3)(z^3/h^2)\right](-8z/h^2)dz,$$
$$I_{SS2ij}=Q_{ij}\int_{+h/2}^{-h/2}\left[z-(16/5)(z^5/h^4)\right](-8z/h^2)dz,\quad I_{SSS1ij}=Q_{ij}\int_{+h/2}^{-h/2}(-8z/h^2)^2dz,$$
$$I_{SSS2ij}=Q_{ij}\int_{+h/2}^{-h/2}(-8z/h^2)f_2''(z)\,dz,\quad J_{ij}=Q_{ij}\int_{+h/2}^{-h/2}\left[z(-64z^3/h^4)\right]dz, \tag{19}$$
$$J_{Sij}=Q_{ij}\int_{+h/2}^{-h/2}z\left[z(-64z^3/h^4)\right]dz,\quad J_{SS1ij}=Q_{ij}\int_{+h/2}^{-h/2}\left[z-(4/3)(z^3/h^2)\right]\left[z(-64z^3/h^4)\right]dz,$$
$$J_{SS2ij}=Q_{ij}\int_{+h/2}^{-h/2}\left[z-(16/5)(z^5/h^4)\right]\left[z(-64z^3/h^4)\right]dz,\quad J_{SSS2ij}=Q_{ij}\int_{+h/2}^{-h/2}\left[z(-64z^3/h^4)\right]^2dz$$

Associated boundary conditions are as:
at $x=0$ and $x=a$

$$N_x=0 \quad \text{or} \quad u_0=0 \tag{20}$$
$$N_{xy}=0 \quad \text{or} \quad v_0=0 \tag{21}$$
$$M_x^b=0 \quad \text{or} \quad w_0=0 \tag{22}$$
$$M_{xy}^b=0 \quad \text{or} \quad \partial w_0/\partial x=0 \tag{23}$$
$$M_x^{S_1}=0 \quad \text{or} \quad \phi_x=0 \tag{24}$$

$$M_x^{S_2}=0 \quad \text{or} \quad \psi_x=0 \tag{25}$$
$$M_{xy}^{S_1}=0 \quad \text{or} \quad \phi_y=0 \tag{26}$$
$$M_{xy}^{S_2}=0 \quad \text{or} \quad \psi_y=0 \tag{27}$$
$$Q_{xz}^{1}=0 \quad \text{or} \quad \phi_z=0 \tag{28}$$
$$Q_{xz}^{2}=0 \quad \text{or} \quad \psi_z=0 \tag{29}$$

at $y=0$ and $y=b$

$$N_{xy}=0 \quad \text{or} \quad u_0=0 \tag{30}$$
$$N_{y}=0 \quad \text{or} \quad v_0=0 \tag{31}$$
$$M_y^{b}=0 \quad \text{or} \quad w_0=0 \tag{32}$$
$$M_{xy}^{b}=0 \quad \text{or} \quad \partial w_0/\partial y=0 \tag{33}$$
$$M_{xy}^{S_1}=0 \quad \text{or} \quad \phi_x=0 \tag{34}$$
$$M_{xy}^{S_2}=0 \quad \text{or} \quad \psi_x=0 \tag{35}$$
$$M_{y}^{S_1}=0 \quad \text{or} \quad \phi_y=0 \tag{36}$$
$$M_{y}^{S_2}=0 \quad \text{or} \quad \psi_y=0 \tag{37}$$
$$Q_{yz}^{1}=0 \quad \text{or} \quad \phi_z=0 \tag{38}$$
$$Q_{yz}^{2}=0 \quad \text{or} \quad \psi_z=0 \tag{39}$$

2.4 Closed-form solutions

A Navier's solution procedure is implemented to obtain static solutions for the FG plates. The displacement variables are assumed to be in the following trigonometric form.

$$\begin{Bmatrix} (u_0,\psi_x,\phi_x) \\ (v_0,\psi_y,\phi_y) \\ (w_0,\psi_z,\phi_z) \end{Bmatrix} = \sum_{m=1,3,5}^{\infty}\sum_{n=1,3,5}^{\infty} \begin{Bmatrix} (u_{mn},\psi_{xmn},\phi_{xmn})\cos\alpha x\sin\beta y \\ (v_{mn},\psi_{ymn},\phi_{ymn})\sin\alpha x\cos\beta y \\ (w_{mn},\psi_{zmn},\phi_{zmn})\sin\alpha x\sin\beta y \end{Bmatrix} \tag{40}$$

where $\alpha = m\pi/a$, $\beta = n\pi/b$ and $u_{mn}, w_{mn}, v_{mn}, \phi_{xmn}, \phi_{ymn}, \psi_{xmn}, \psi_{ymn}, \phi_{zmn}, \phi_{zmn}$ are the unknown coefficients. The transverse load is also considered to be in trigonometric form.

$$q(x,y)=\sum_{m=1,3,5}^{\infty}\sum_{n=1,3,5}^{\infty} q_{mn}\sin\alpha x\,\sin\beta y \tag{41}$$

The Fourier coefficients (q_{mn}) for different loading conditions are as follows,

$$q_{mn}=q_0 \quad (m=1,\ n=1)\ \text{(Sinusoidal distributed load)} \tag{42}$$
$$q_{mn}=\frac{16q_0}{mn\pi^2} \quad (m=1, 3, 5\ldots n=1, 3, 5\ldots)\quad \text{(Uniformly distributed load)} \tag{43}$$

where q_0 is the maximum intensity. Substituting Eqs. (40)-(43) into the Eqs. (11)-(18) leads to the following equations:

$$[K]\{\Delta\}=\{Q\} \tag{44}$$

where the elements of Matrix K are described in the Appendix and also we have:

$$\begin{aligned} \{Q\} &= \{0,0,q_{mn},0,0,0,0,0,0\} \\ \{\Delta\} &= \{u_{mn},v_{mn},w_{mn},\phi_{xmn},\psi_{xmn},\phi_{ymn},\psi_{ymn},\phi_{zmn},\psi_{zmn}\}^T \end{aligned} \tag{45}$$

3. Illustrative examples and validation

The bending analysis of the FG plates is presented herein to prove validity of the theory. The properties of the metal and ceramic are; Metal: E_m= 70 *GPa* and μ = 0.3, Ceramic: E_c = 380 *GPa* and μ = 0.3. The non-dimensional quantities are presented in the following form.

Isotropic Plate:

$$\bar{w}\left(\frac{a}{2},\frac{b}{2},0\right)=\frac{100Eh^3}{q_0\,a^4}w,\quad \bar{\sigma}_x\left(\frac{a}{2},\frac{b}{2},-\frac{h}{2}\right)=\frac{h^2}{q_0a^2}\sigma_x,\ \bar{\tau}_{xz}\left(\frac{a}{2},0,\frac{z}{h}\right)=\frac{h}{q_0a}\tau_{xz} \tag{46}$$

FG Plate:

$$\bar{w}\left(\frac{a}{2},\frac{b}{2},0\right)=\frac{100E_ch^3}{q_0\,a^4}w,\quad (\bar{\sigma}_x,\bar{\sigma}_y)\left(\frac{a}{2},\frac{b}{2},-\frac{h}{2}\right)=\frac{h}{q_0a}(\sigma_x,\sigma_y),$$
$$\bar{\tau}_{xy}\left(0,0,-\frac{h}{2}\right)=\frac{h}{q_0a}\tau_{xy},\ \bar{\tau}_{xz}\left(\frac{a}{2},0,\frac{z}{h}\right)=\frac{h}{q_0a}\tau_{xz},\ \bar{\tau}_{yz}\left(0,\frac{b}{2},\frac{z}{h}\right)=\frac{h}{q_0a}\tau_{yz} \tag{47}$$

3.1 Validation and discussion of results

Due to the unavailability of the exact 3D solutions for FG plates, the present FOSNDT is applied to isotropic plates (E =210 GPa, μ = 0.3) to prove its accuracy and validity. Non-dimensional quantities are shown in Table 1. Exact solution of Pagano [52], CPT of Kirchhoff [53], FSDT of Mindlin [54], parabolic shear deformation theory (PSDT) of Reddy [55], and sinusoidal shear and normal deformation plate theory (SSNPT) of Sayyad and Ghugal [56] are used for the comparison purpose. The CPT neglects the shear effect, the FSDT considers the first-order shear effect, the PSDT considers the third-order shear effect. SSNPT considers the sinusoidal type shear effect. In the comparison of these theories, the present theory considers the fifth-order shear effect along with thickness stretching effect. Table 1 shows that the present FOSNDT yields accurate predictions of displacements and stresses for all aspect ratios compared to other well-known plate theories. This is mainly due to the inclusion of fifth-order variation of displacements and thickness stretching effect. In many cases, percentage error predicted by the FOSNDT is lower than other existing plate theories. For a/h = 4, the percentage error in transverse deflection predicted by the present theory is 0.076% whereas PSDT, SSNPT, FSDT, and CPT show error of 3.380, -0.262, -1.010, 23.47 %, respectively. A similar type of error difference can be observed for in-plane normal and transverse shear stresses. CPT and FSDT show higher percentage error in the prediction due to the neglect of the effects of normal strains. Therefore, it is revealed that the FOSNDT is more accurate compared to the other theories.

Table 1. Non-dimensional deflection and stresses for the isotropic square plate subjected to sinusoidal load (a=b).

a/h	Model	$\bar{w}(0)$	% error	$\bar{\sigma}_x(h/2)$	% error	$\bar{\tau}_{xz}(0)$	% error
4	Present (FOSNDT)	3.6658	**0.076**	0.2060	**-0.980**	0.2356	**-0.211**
	PSDT [55]	3.7870	3.380	0.2090	-2.450	0.2260	-4.277
	SSNPT [56]	3.6534	-0.262	0.2267	-11.12	0.2355	-0.254
	FSDT [54]	3.6260	-1.010	0.1970	-3.430	0.2390	1.220
	CPT [53]	2.8030	23.47	0.1970	-3.430	0.2380	0.804
	Exact [52]	3.6630	00.00	0.2040	00.00	0.2361	0.000
10	Present (FOSNDT)	2.9491	**0.224**	0.2000	**0.855**	0.2383	**0.000**
	PSDT [55]	2.9610	6.280	0.1990	0.100	0.2290	3.900
	SSNPT [56]	2.9333	0.397	0.2125	6.890	0.2380	-0.126
	FSDT [54]	2.9340	2.888	0.1970	-0.905	0.2390	0.293
	CPT [53]	2.8020	4.770	0.1970	-0.905	0.2380	-0.419
	Exact [52]	2.9425	00.00	0.1988	00.00	0.2383	0.000
20	Present (FOSNDT)	2.8412	**0.123**	0.1986	**0.353**	0.2387	**0.000**
	PSDT [55]	2.8286	-0.320	0.2105	6.360	0.2384	-0.125
	SSNPT [56]	2.8377	00.00	0.1979	00.00	0.2387	0.000
	FSDT [54]	2.8109	**0.096**	0.1981	**0.253**	0.2387	**0.041**
	CPT [53]	2.7991	-0.324	0.2100	6.270	0.2385	-0.041
	Exact [52]	2.8082	00.00	0.1976	00.00	0.2386	0.000
100	Present (FOSNDT)	2.8066	**0.092**	0.1976	**0.000**	0.2388	**0.041**
	PSDT [55]	2.8040	0.000	0.1980	0.202	0.2390	0.125
	SSNPT [56]	2.7949	-0.324	0.1980	0.202	0.2385	-0.041
	FSDT [54]	2.8040	0.000	0.1980	0.202	0.2390	0.125
	CPT [53]	2.8030	-0.035	0.1980	0.202	0.2390	0.125
	Exact [52]	2.8040	00.00	0.1976	00.00	0.2387	0.000

Table 2 presents values of non-dimensional quantities of FGM plate for p = {0, 1, 5, 10} and a/h = 10. The top surface, i.e. metal surface, is subjected to mechanical load. The present results are compared with those presented by PSDT of Reddy [55], trigonometric, hyperbolic, and exponential shear deformation theories (TSDT, HSDT, and ESDT) developed by Sayyad and Ghugal [56], Mindlin [54] and Kirchhoff [53]. It is observed from Table 2 that PSDT, TSDT, HSDT, and ESDT overestimate the results for FG plate under sinusoidal load. This is in fact due to the neglect of transverse normal deformations, i.e. thickness stretching effect. It is important to note that the nondimensional displacements and stresses are increasing with growth in the power-law index. This is due to increases in the power-law index which reduces the stiffness of the plate. Distributions of stresses in z-direction are plotted in Fig. 3. From these figures, it is observed that the variations of in-plane normal and shear stresses ($\bar{\sigma}_x, \bar{\tau}_{xy}$) are linear for p = 0 and nonlinear for p = {1, 5, 10}. It is also observed from Fig. 3 that the maximum compressive in-plane normal stress is increased with an increase in the power-law index. Moreover, it is observed that the transverse shear stresses are maximum at mid-plane (z/h = 0) when $\boldsymbol{p}$ = 0 and maximum at z = +0.14h and +0.22h when p = 1 and 5, respectively. This is due to the fact that mid-plane shifted toward ceramic face due to an increase in power-law index.

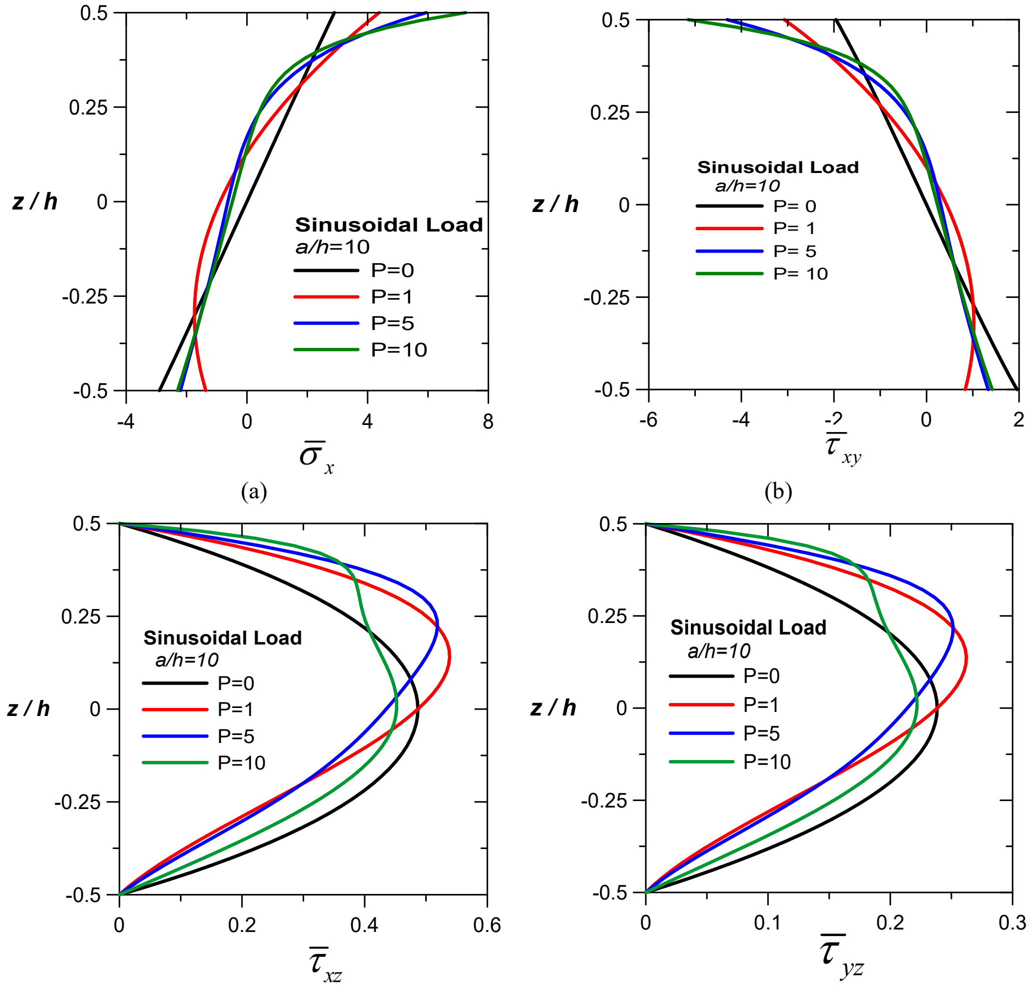

(c) (d)

Fig. 3. Distribution of stresses in z-direction for sinusoidal load

Table 2. Non-dimensional deflection and stresses for the functionally graded square plate subjected to sinusoidal load (a=b and a/h=10)

P	Model	$\bar{w}(0)$	$\bar{\sigma}_x(h/2)$	$\bar{\sigma}_y(h/2)$	$\bar{\tau}_{xy}(h/2)$	$\bar{\tau}_{xz}(0)$	$\bar{\tau}_{yz}(0)$
0	Present (FOSNDT)	2.9425	1.9964	1.9964	1.0634	0.2384	0.2384
	PSDT [55]	2.9606	1.9943	1.9943	1.0739	0.2386	0.2386
	TSDT [29]	2.9603	1.9955	1.9955	1.0745	0.2462	0.2462
	HSDT [29]	2.9595	1.9937	1.9937	1.0735	0.2371	0.2371
	ESDT [29]	2.9575	1.9967	1.9967	1.0752	0.2437	0.2437
	FSDT [54]	2.9343	1.9758	1.9758	1.0639	0.1592	0.1592
	CPT [53]	2.8026	1.9758	1.9758	1.0639	---	---
1	Present (FOSNDT)	5.6956	3.0605	3.0605	1.6715	0.2604	0.2604
	PSDT [55]	5.8895	3.0850	3.0850	1.6612	0.2623	0.2623
	TSDT [29]	5.8891	3.0870	3.0870	1.6622	0.2667	0.2667
	HSDT [29]	5.8895	3.0848	3.0848	1.6611	0.2619	0.2619
	ESDT [29]	5.8878	3.0889	3.0889	1.6632	0.2717	0.2717
	FSDT [54]	5.8452	3.0536	3.0536	1.6443	0.2688	0.2688
	CPT [53]	5.6228	3.0536	3.0536	1.6443	---	---
5	Present (FOSNDT)	8.7493	4.1880	4.1880	2.3219	0.2511	0.2511
	PSDT [55]	9.1135	4.2447	4.2447	2.2856	0.2659	0.2659
	TSDT [29]	9.1183	4.2488	4.2488	2.2878	0.2574	0.2574
	HSDT [29]	9.1130	4.2443	4.2443	2.2854	0.2668	0.2668
	ESDT [29]	9.1210	4.2527	4.2527	2.2899	0.2514	0.2514
	FSDT [54]	8.9321	4.1848	4.1848	2.2534	0.4971	0.4971

Table 2. Continued

	CPT [53]	8.5207	4.1848	4.1848	2.2534	---	---
10	Present (FOSNDT)	9.8204	5.0845	5.0845	2.7841	0.2218	0.2218
	PSDT [55]	10.087	5.0849	5.0849	2.7380	0.2115	0.2115
	TSDT [29]	10.089	5.0890	5.0890	2.7402	0.2198	0.2198
	HSDT [29]	10.086	5.0845	5.0845	2.7378	0.2107	0.2107
	ESDT [29]	10.088	5.0928	5.0928	2.7423	0.2282	0.2282
	FSDT [54]	9.8644	5.0173	5.0173	2.7016	0.6160	0.6160
	CPT [53]	9.3546	5.0173	5.0173	2.7016	---	---

Table 3 shows comparison of non-dimensional displacements and stresses of FGM plate subjected to uniformly distributed load (UDL). Similar trends in results and distributions of stresses (see Fig. 4) are observed when the plate is loaded UDL.

Figure 5 illustrates the variation of transverse normal stress ($\bar{\sigma}_z$) across the thickness of the plate. This variation is rarely available in the whole variety of literature due to the neglect of transverse normal effect. Variations of transverse deflection with respect to aspect ratio are plotted in Fig. 6. Examination of Fig. 6 displays that the non-dimensional transverse deflection is increased with the increase in the power-law index. Moreover, values of transverse deflection are almost constant for higher values of *a/h* ratios i.e. for thin plates.

Table 3. Non-dimensional deflection and stresses for the functionally graded square plate subjected to uniformly distributed load (UDL) ($a=b$ and $a/h=10$).

P	Model	$\bar{w}(0)$	$\bar{\sigma}_x(h/2)$	$\bar{\sigma}_y(h/2)$	$\bar{\tau}_{xy}(h/2)$	$\bar{\tau}_{xz}(0)$	$\bar{\tau}_{yz}(0)$
0	Present (FOSNDT)	4.6397	2.8961	2.8961	1.9541	0.4868	0.4868
	PSDT [55]	4.6659	2.8928	2.8928	2.0331	0.4925	0.4925
	TSDT [29]	4.6655	2.8940	2.8940	1.9964	0.5077	0.5077
	HSDT [29]	4.6643	2.8921	2.8921	1.9264	0.4890	0.4890
	ESDT [29]	4.6615	2.8943	2.8943	2.0176	0.5023	0.5023
	FSDT [54]	4.6277	2.8735	2.8735	1.9473	0.3300	0.3300
	CPT [53]	4.4361	2.8735	2.8735	1.9473	---	---
1	Present (FOSNDT)	8.9852	4.4190	4.4190	3.0724	0.5335	0.5335
	PSDT [55]	9.2880	4.4738	4.4738	3.1724	0.5414	0.5414
	TSDT [29]	9.2874	4.4758	4.4758	3.0927	0.5501	0.5501
	HSDT [29]	9.2880	4.4736	4.4736	2.9771	0.5407	0.5407
	ESDT [29]	9.2856	4.4777	4.4777	3.1654	0.5598	0.5598
	FSDT [54]	9.2234	4.4411	4.4411	3.0097	0.5574	0.5574
	CPT [53]	8.9000	4.4411	4.4411	3.0097	---	---
5	Present (FOSNDT)	13.777	6.0400	6.0400	4.3034	0.5166	0.5166
	PSDT [55]	14.349	6.1484	6.1484	4.3737	0.5480	0.5480
	TSDT [29]	14.356	6.1526	6.1526	4.2816	0.5298	0.5298
	HSDT [29]	14.348	6.1480	6.1480	4.0138	0.5499	0.5499
	ESDT [29]	14.360	6.1565	6.1565	4.3615	0.5167	0.5167
	FSDT [54]	14.085	6.0862	6.0862	4.1245	1.0307	1.0307
	CPT [53]	13.486	6.0862	6.0862	4.1245	---	---
10	Present (FOSNDT)	15.457	7.3217	7.3217	5.1493	0.4522	0.4522
	PSDT [55]	15.872	7.3672	7.3672	5.2118	0.4357	0.4357
	TSDT [29]	15.875	7.3713	7.3713	5.1209	0.4524	0.4524
	HSDT [29]	15.872	7.3668	7.3668	4.7875	0.4343	0.4343
	ESDT [29]	15.874	7.3751	7.3751	5.1953	0.4690	0.4690
	FSDT [54]	15.548	7.2970	7.2970	4.9450	1.2773	1.2773
	CPT [53]	14.806	7.2970	7.2970	4.9450	---	---

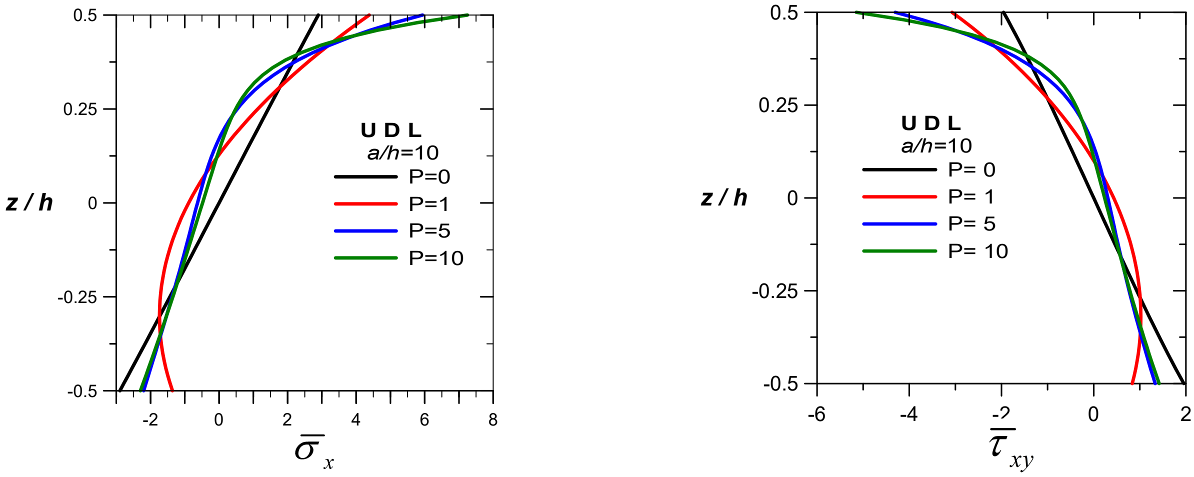

(a) (b)

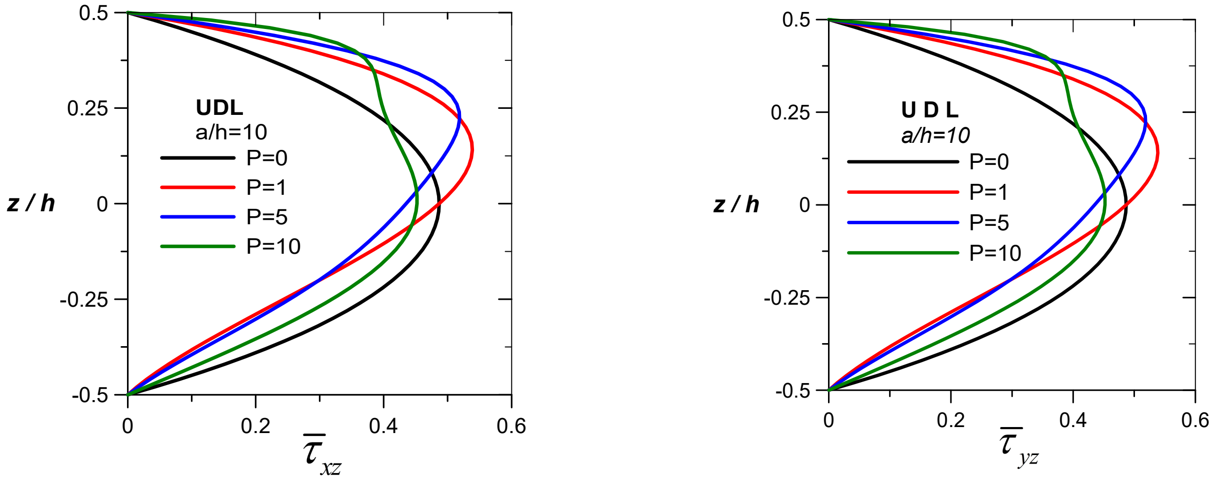

(c) (d)

Fig. 4. Distribution of stresses in z-direction for the FG plate under UDL

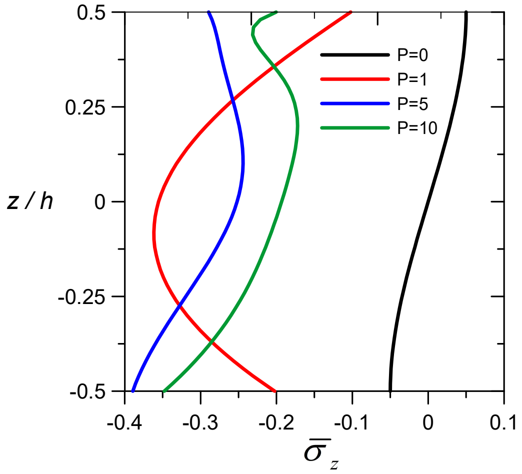

Fig. 5. Distribution of ($\bar{\sigma}_z$) in z-direction for sinusoidal load

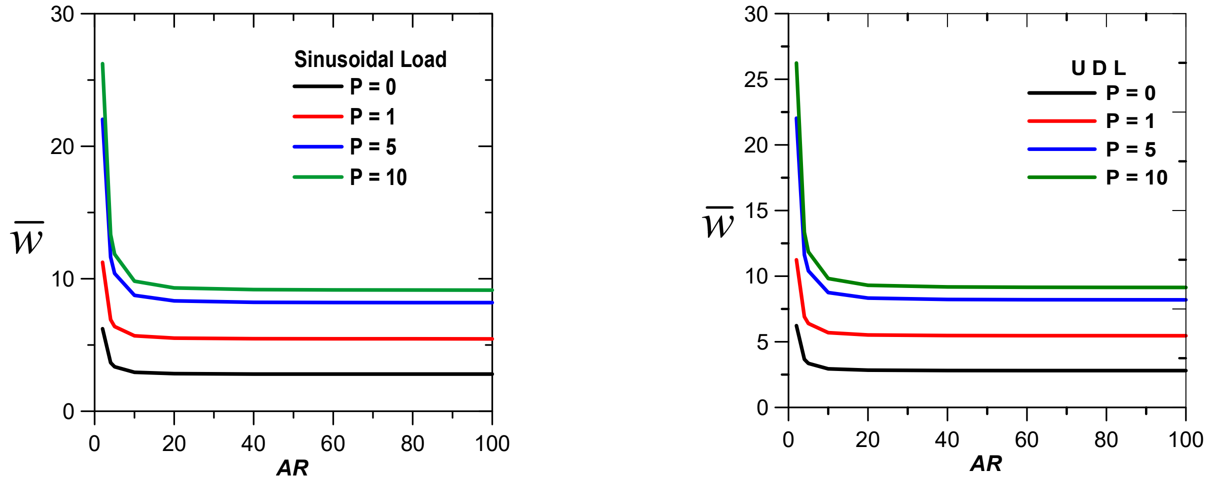

(a) (b)

Fig. 6. Variation of non-dimensional transverse displacement ($\bar{w}$) with respect to the different aspect ratios

4. Conclusions

A new quasi-3D fifth-order displacement based model was developed and presented for the bending analysis of FGM plates. The theory considered the effects of transverse normal strain/stress on the bending of a plate. Governing equations were obtained using the principle of virtual work. Closed-form solutions were presented based on Navier's technique. Numerical results were presented when the plate is subjected to sinusoidal and distributed loads. From the numerical study and discussion of the results following conclusions were drawn.

1) The present theory yields accurate predictions of displacements and stresses compared to other well-known higher order plate theories. This is mainly due to the inclusion of fifth-order variation of displacements and thickness stretching effect.
2) It is deduced that the non-dimensional displacements and stresses are increasing with an increase in the power-law index. This is due to the increases in power-law index which reduces stiffness of the plate and increases its flexibility.
3) It is concluded that the variations of in-plane normal and shear stresses are linear for $p = 0$ and nonlinear for higher values of the power-law index due to gradation of material properties.
4) It is also concluded that mid-plane of the plate is shifted towards ceramic face due to an increase in power-law index.

Overall, it is concluded that the present theory is accurate and strongly recommended for the bending analysis of FGM plate.

Conflict of Interest

The author(s) declared no potential conflicts of interest with respect to the research, authorship and publication of this article.

Funding

The author(s) received no financial support for the research, authorship and publication of this article.

References

[1] Jha, D. K., Kant, T., Singh, R. K., A critical review of recent research on functionally graded plates, *Composite Structures*, 96, 2013, 833-849.
[2] Swaminathan, K., Naveenkumar, D. T., Zenkour, A. M., Carrera, E., Stress, vibration and buckling analyses of FGM plates-A state-of-the-art review, *Composite Structures*, 120, 2015, 10-31.
[3] Swaminathan, K., Sangeetha, D. M., Thermal analysis of FGM plates-A critical review of various modeling technique and solution methods, *Composite Structures*, 160, 2017, 43-60.
[4] Sayyad, A. S., Ghugal, Y. M., On the free vibration analysis of laminated composite and sandwich beams: A review of recent literature with some numerical results, *Composite Structures,* 129, 2015, 177–201.
[5] Sayyad, A. S., Ghugal, Y. M., Bending, buckling and free vibration of laminated composite and sandwich plates: A critical review of literature, *Composite Structures*, 171, (2017a), 486–504.
[6] Reddy, J. N., Analysis of functionally graded plates, *International Journal of Numerical Methods in Engineering,* 47, 2000, 663-684.
[7] Reddy, J. N., Cheng, Z. Q., Frequency of functionally graded plates with three-dimensional asymptotic approach, *ASCE Journal of Engineering Mechanics,* 129, 2003, 896-900.
[8] Zenkour, A. M., Generalized shear deformation theory for bending analysis of functionally graded plates, *Applied Mathematical Modelling*, 30, 2006, 67-84.
[9] Zhong, Z., Shang, E., Closed-form solutions of three-dimensional functionally graded plates, *Mechanics of Advanced Materials and Structures*, 15, 2008, 353-363.
[10] Lu, C. F., Lim, W., Chen, W. Q., Exact solutions for free vibrations of functionally graded thick plates on elastic foundations, *Mechanics of Advanced Materials and Structures*, 16, 2009, 576-584.
[11] Ameur, M., Tounsi, A., Mechab, I., Bedia, E. A. A., A new trigonometric shear deformation theory for bending analysis of functionally graded plates resting on elastic foundations*, KSCE Journal of Civil Engineering*, 15, 2011, 1405-1414.
[12] Jha, D. K., Kant, T., Singh, R. K., Stress analysis of transversely loaded functionally graded plates with a higher order shear and normal deformation theory, *ASCE Journal of Engineering Mechanics*, 139, 2013, 1663-1680.
[13] Neves, A. M. A., Ferreira, A. J. M., Carrera, E. M., Cinfera, M., Jorge, R., Static, free vibration and buckling analysis of functionally graded plates using a quasi-3D higher-order shear deformation theory and a meshless technique*, Composite Structures*, 44, 2013, 657-674.
[14] Thai, H. T., Choi, D. H., Levy solution for free vibration analysis of functionally graded plates based on a refined plate theory, *KSCE Journal of Civil Engineering*, 8(6), 2014, 1813-1824.
[15] Najafizadeh, M. M., Mohammadi, J., Khazaeinejad, P., Vibration characteristics of functionally graded plates with non-ideal boundary conditions, *Mechanics of Advanced Materials and Structures*, 19, 2012, 543-550.
[16] Neves, A. M. A., Ferreira, A. J. M., Carrera, E., Cinefra, A., Roque, C. M. C., Jorge, R. M. N., Soares, C. M. M., A quasi-3D hyperbolic shear deformation theory for the static and free vibration analysis of functionally graded plates. *Composite Structures,* 94, 2012, 1814-1825.
[17] Thai, H. T., Thuc, P. V., A new sinusoidal shear deformation theory for bending, buckling and vibration of functionally graded plates, *Applied Mathematical Modelling*, 37, 2013, 3269-3281.
[18] Thai, H. T., Kim, S. E., A simple higher-order shear deformation theory for bending and free vibration analysis of functionally graded plates, *Composite Structures*, 96, 2013, 165-17.
[19] Mechab, I., Mechab, B., Benaissa, S., Static and dynamic analysis of functionally graded plates using four-variable refined plate theory by the new function, *Composites Part-B* 45,2013,748-757.
[20] Thai, H. T., Choi, D. H., Levy solution for free vibration analysis of functionally graded plates based on a refined plate theory, *KSCE Journal of Civil Engineering*, 8(6), 2014, 1813-1824.

[21] Reddy, K. S. K., Kant, T., Three-dimensional elasticity solution for free vibrations of exponentially graded plates, *Journal of Engineering Mechanics*, 140, 2014, 1-9.
[22] Thai, H. T., Choi, D. H., Levy solution for free vibration analysis of functionally graded plates based on a refined plate theory, *KSCE Journal of Civil Engineering*, 8(6), 2014, 1813-1824.
[23] Hadaji, L., Khelifa, Z., Abbes, A. B. E., A new higher order shear deformation model for functionally graded beams, *KSCE Journal Civil Engineering*, 20, 2016, 1835–1841.
[24] Mantari, J. L., Ramos, I. A., Carrera, E., Petrolo, M., Static analysis of functionally graded plates using new non polynomial displacement fields via Carrera unified formulation, *Composites Part-B*, 89, 2016, 127–142.
[25] Amirpour, M., Das, R., Flores, E. I., Analytical solutions for elastic deformation of functionally graded thick plates with in-plane stiffness variation using higher order shear deformation theory, *Composite Structures*, 94, 2016, 109–121.
[26] Thai, C. H., Zenkour, A. M., Wahab, M. A., Xuan, H. N., A four unknown shear and normal deformation theory for functionally graded isotropic and sandwich plate based on isogeometric analysis, *Composites Part-B,* 139, 2016, 77-95.
[27] Li, L., Zhang, D. G., Free vibration analysis of rotating functionally graded rectangular plates, *Composite Structures*, 136, 2016, 493-504.
[28] Park, M., Choi, D. H., A simplified first-order shear deformation theory for bending, buckling and free vibration analyses of isotropic plates on elastic foundations, *KSCE Journal of Civil Engineering*, 22(4), 2017, 1235-1249.
[29] Sayyad, A. S., Ghugal, Y. M., A unified shear deformation theory for the bending of isotropic, functionally graded, laminated and sandwich beams and plates, *International Journal of Applied Mechanics*, 9(1), 2017, 1-36.
[30] Naik, N. S., Sayyad, A. S., 1D analysis of laminated composite and sandwich plates using a new fifth-order plate theory. *Latin American Journal of Solids and Structures,* 15, 2018, 1-17.
[31] Sayyad, A. S., Ghugal, Y. M., Modeling and analysis of functionally graded sandwich beams: A review, *Mechanics of Advanced Materials and Structures*, (In Press) DOI: 10.1080/15376494.2018.1447178.
[32] Akbas, S. D., Vibration and static analysis of functionally graded porous plates, *Journal of Applied and Computational Mechanics*, 3(3), 2017, 199-207.
[33] Zenkour, A. M., A quasi-3D refined theory for functionally graded single-layered and sandwich plates with porosities, *Composite Structures*, 201, 2018, 38-48.
[34] Avcar, M., Mohammed W. K. M., Free vibration of functionally graded beams resting on Winkler-Pasternak foundation, *Arabian Journal of Geosciences*, 11 (10), 2018, 1-8.
[35] Avcar, M., Alwan, H. H. A., Free vibration of functionally graded Rayleigh beam, *International Journal of Engineering & Applied Sciences*, 9(2), 2017, 127-137.
[36] Sobhy, M., Radwan, A. F., A new quasi 3D nonlocal plate theory for vibration and buckling of FGM nanoplates, *International Journal of Applied Mechanics*, 9(1), 2017, 1-29.
[37] Avcar, M., Effects of rotary inertia shear deformation and non-homogeneity on frequencies of beam, *Structural Engineering and Mechanics*, 55 (4), 2015, 871-884.
[38] Hebali, H., Tounsi, A., Houari, M. S. A., Bessaim, A., Bedia, E. A. A., New quasi-3D hyperbolic shear deformation theory for the static and free vibration analysis of functionally graded plates, *Journal of Engineering Mechanics,* 140, 2014, 374-383.
[39] Mercan, K., Baltacıoglu, A. K., Civalek, O., Free vibration of laminated and FGM/CNT composites annular thick plates with shear deformation by discrete singular convolution method, *Composite Structures*, 186, 2018, 139-153.
[40] Akbas, S. D., Stability of a non-homogenous porous plate by using generalized differential quadrature method, *International Journal of Engineering and Applied Sciences*, 9, 2017, 147-155.
[41] Akbas, S. D., Thermal effects on the vibration of functionally graded deep beams with porosity, *International Journal of Applied Mechanics*, 9(5), 2017, 1-18.
[42] Akbas, S. D., On post-buckling behavior of edge cracked functionally graded beams under axial loads, *International Journal of Structural Stability and Dynamics*, 15 (4), 2015, 1-21.
[43] Akbas, S. D., Post-buckling analysis of axially functionally graded three-dimensional beams, *International Journal of Applied Mechanics*, 7 (3), 2015, 1-20.
[44] Ersoy, H., Mercan, K., Civalek, O., Frequencies of FGM shells and annular plates by the methods of discrete singular convolution and differential quadrature methods, *Composite Structures*, 183, 2018, 7-20.
[45] Nasihatgozar, M., Khalili S. M. R., Free vibration of a thick sandwich plate using higher order shear deformation theory and DQM for different boundary conditions, *Journal of Applied and Computational Mechanics*, 3, 2017, 16-24.
[46] Dastjerdi, S., Akgoz, B., New static and dynamic analyses of macro and nano FGM plates using exact three-dimensional elasticity in thermal environment, *Composite Structures,* 192, 2018, 626-641.
[47] Civalek, O., Free vibration of carbon nanotubes reinforced (CNTR) and functionally graded shells and plates based on FSDT via discrete singular convolution method, *Composites Part B: Engineering*, 111, 2017, 45-59.
[48] Civalek, O., Nonlinear dynamic response of laminated plates resting on nonlinear elastic foundations by the discrete singular convolution-differential quadrature coupled approaches, *Composites Part B: Engineering*, 50, 2013, 171–179.
[49] Civalek, O., Three-dimensional vibration, buckling and bending analyses of thick rectangular plates based on discrete singular convolution method, *International Journal of Mechanical Sciences*, 49 (6), 2007, 752-765.
[50] Akgoz, B., Civalek, O., Nonlinear vibration analysis of laminated plates resting on nonlinear two parameters elastic foundations, *Steel and Composite Structures*, 11 (5), 403-421.

[51] Ghumare, S. M., Sayyad, A. S., A new fifth order shear and normal deformation theory for static bending and elastic buckling of P-FGM beams, *Latin American Journal of Solids and Structures*, 14, 2017, 1893-1911.
[52] Pagano, N. J., Exact solution for composite laminates in cylindrical bending, *Journal of Composite Materials*, 3, 1969, 398-411.
[53] Kirchhoff, G. R., Uber das gleichgewicht und die bewegung einer elastischen Scheibe, *International Journal of Pure Applied Mathematics*, 40, 1850, 51-88.
[54] Mindlin, R. D., Influence of rotatory inertia and shear on flexural motions of isotropic, elastic plates, *ASME Journal of Applied Mechanics*, 18, 1951, 31-38.
[55] Reddy, J. N., A simple higher order theory for laminated composite plates. *Journal of Applied Mechanics,* 51, 1984, 745-752.
[56] Sayyad, A. S., Ghugal, Y. M., A new shear and normal deformation theory for isotropic, transversely isotropic, laminated composite and sandwich plates, *International Journal of Mechanics and Materials in Design*, 3, 2014, 247–267.
[57] Sayyad, A. S., Ghugal, Y. M., Bending of shear deformable plates resting on Winkler foundations according to trigonometric plate theory, *Journal of Applied and Computational Mechanics*, 4(3), 2018, 187-201.

Appendix

$$K_{11}=-(A_{11}\alpha^2+A_{66}\beta^2),\quad K_{12}=-(A_{12}+A_{66})\alpha\beta,\quad K_{13}=B_{11}\alpha^3+B_{12}\alpha\beta^2+2B_{66}\alpha\beta^2,$$

$$K_{14}=-(C_{11}\alpha^2+C_{66}\beta^2),\quad K_{15}=-(D_{11}\alpha^2+D_{66}\beta^2),\quad K_{16}=-(C_{12}+C_{66})\alpha\beta,$$

$$K_{17}=-(D_{12}+D_{66})\alpha\beta,\quad K_{18}=I_{13}\alpha,\quad K_{19}=J_{13}\alpha,\quad K_{22}=-(A_{66}\alpha^2+A_{12}\beta^2),$$

$$K_{23}=B_{12}\alpha^2\beta+2B_{66}\alpha^2\beta+B_{22}\beta^3,\quad K_{24}=-(C_{12}+C_{66})\alpha\beta,\quad K_{25}=-(D_{12}+D_{66})\alpha\beta,$$

$$K_{26}=-(C_{22}\beta^2+C_{66}\alpha^2),\quad K_{27}=-(D_{22}\beta^2+D_{66}\alpha^2),\quad K_{28}=I_{23}\beta, K_{29}=J_{23}\beta,$$

$$K_{33}=-(A_{S11}\alpha^4+2A_{S12}\alpha^2\beta^2+A_{S22}\beta^4+4A_{s66}\alpha^2\beta^2),\quad K_{34}=C_{S11}\alpha^3+C_{S12}\alpha\beta^3+2C_{S66}\alpha\beta^2,$$

$$K_{35}=D_{S11}\alpha^3+D_{S12}\alpha\beta^2+2D_{S66}\alpha\beta^2,\quad K_{36}=C_{S12}\alpha^2\beta+C_{S22}\beta^3+2C_{S66}\alpha^2\beta,$$

$$K_{37}=D_{S12}\alpha^2\beta+D_{S22}\beta^3+2D_{S66}\alpha^2\beta,\quad K_{38}=-(I_{S13}\alpha^2+I_{S23}\beta^2),\quad K_{39}=-(J_{S13}\alpha^2+J_{S23}\beta^2),$$

$$K_{44}=-(C_{SS111}\alpha^2+C_{SS166}\beta^2+C_{SSS144}),\quad K_{45}=-(C_{SS211}\alpha^2+C_{SS266}\beta^2+C_{SSS244}),$$

$$K_{46}=-(C_{SS112}+C_{SS166})\alpha\beta,\quad K_{47}=-(C_{SS212}+C_{SS266})\alpha\beta,\quad K_{48}=(I_{SS113}-C_{SSS144})\alpha,$$

$$K_{49}=(J_{SS113}-D_{SSS144})\alpha,\quad K_{55}=-(D_{SS211}\alpha^2+D_{SS266}\beta^2+D_{SSS244}),\quad K_{56}=-(C_{SS212}+C_{SS266})\alpha\beta,$$

$$K_{57}=-(D_{SS212}+D_{SS266})\alpha.\beta,\quad K_{58}=(I_{SS213}-C_{SSS244})\alpha,\quad K_{59}=(J_{SS213}-D_{SSS244})\alpha,$$

$$K_{66}=-(C_{SS122}\beta^2+C_{SS166}\alpha^2+C_{SSS155}),\quad K_{67}=-(C_{SS222}\beta^2+C_{SS266}\alpha^2+C_{SSS255}),$$

$$K_{68}=(I_{SS123}-C_{SSS155})\beta,\quad K_{69}=(J_{SS123}-C_{SSS255})\beta,\quad K_{77}=-(D_{SS222}\beta^2+D_{SS266}\alpha^2+D_{SSS255}),$$

$$K_{78}=(I_{SS233}-C_{SSS255})\beta,\quad K_{79}=(J_{SS233}-D_{SSS255})\beta,\quad K_{88}=-(C_{SSS144}\alpha^2+C_{SS155}\beta^2+I_{SSS133}),$$

$$K_{89}=-(C_{SSS244}\alpha^2+C_{SS255}\beta^2+I_{SSS233}),\quad K_{99}=-(D_{SSS244}\alpha^2+D_{SSS255}\beta^2-J_{SSS233}),$$

$$K_{21}=K_{12},\ K_{31}=K_{13},\ K_{41}=K_{14},\ K_{51}=K_{15},\ K_{61}=K_{16}, K_{71}=K_{17}, K_{81}=K_{18}, K_{91}=K_{19},$$

$$K_{32}=K_{23},\ K_{42}=K_{24},\ K_{52}=K_{25},\ K_{62}=K_{26},\ K_{72}=K_{27}, K_{82}=K_{28}, K_{92}=K_{29}, K_{43}=K_{34},$$

$$K_{53}=K_{35},\ K_{63}=K_{36},\ K_{73}=K_{37},\ K_{83}=K_{38},\ K_{93}=K_{39}, K_{54}=K_{45}, K_{64}=K_{46}, K_{74}=K_{47},$$

$$K_{84}=K_{48},\ K_{94}=K_{49},\ K_{65}=K_{56},\ K_{75}=K_{57},\ K_{85}=K_{58}, K_{95}=K_{59}, K_{76}=K_{67}, K_{86}=K_{68},$$

$$K_{96}=K_{69},\quad K_{87}=K_{78},\quad K_{97}=K_{79},\quad K_{98}=K_{89}$$